

1 **The last *r* locus unveiled: T4 RIII is a cytoplasmic co-antiholin**

2

3 Yi Chen ^{a,b} and Ry Young ^{a,b#}

4

5

6

7 Department of Biochemistry and Biophysics, Texas A&M University, College Station,

8 Texas ^a

9 Center for Phage Technology, Texas A&M University, College Station, Texas ^b

10

11

12 **Running title:** T4 RIII is a co-antiholin

13

14

15 #Address correspondence to Ry Young, ryland@tamu.edu, Phone: 979-845-2087, Fax:

16 979-862-4718

17

18

19

20

21

22

23

24 **Abstract**

25 The latent period of phage T4, normally ~25 min, can be extended indefinitely if
26 the infected cell is super-infected after 5 min. This phenomenon, designated as lysis
27 inhibition (LIN), was first described in the 1940s and genetically defined by mutations in
28 diverse T4 *r* genes. RI, the main effector of LIN, was shown to be secreted to the
29 periplasm where, upon activation by super-infection with a T-even virion, it binds to the
30 C-terminal periplasmic domain of the T4 holin T, and blocks its lethal permeabilization of
31 the cytoplasmic membrane. Another *r* locus, *rIII*, has been the subject of conflicting
32 reports. Here we show that RIII, an 82 amino acid protein, is also required for LIN in
33 both *Escherichia coli* B strains and K-12 strains. In T4 Δ *rIII* infections, LIN was briefly
34 established but was unstable. The overexpression of a cloned *rIII* gene alone impeded
35 T-mediated lysis temporarily. However, co-expression of *rIII* and *rl* resulted in a stable
36 LIN state. Bacterial two-hybrid assays and pull-down assays showed that RIII interacts
37 with the cytoplasmic N-terminus of T, which is a critical domain for holin function. We
38 conclude that RIII is a T4 antiholin which blocks membrane hole-formation by directly
39 interacting with the holin. Accordingly, we propose an augmented model for T4 LIN that
40 involves the stabilization of a complex of three proteins in two compartments of the cell:
41 RI interacting with the C-terminus of T in the periplasm and RIII interacting with the N-
42 terminus of T in the cytoplasm.

43

44

45

46

47 **Importance**

48 Lysis inhibition is a unique feature of phage T4 in response to environmental conditions,
49 effected by the antiholin RI, which binds to the periplasmic domain of the T holin and
50 blocks its hole-forming function. Here we report that T4 gene *rIII* encodes a cytoplasmic
51 antiholin which inhibits holin T, together with the main antiholin RI, by forming a complex
52 of three proteins spanning two cell compartments.

53

54 **Introduction**

55 The *r* genes of the T-even phages, first identified by laboratories of the Phage
56 Group in the 1940s (1, 2), have a special place in the history of molecular biology.
57 Detailed studies of the first three loci discovered, - *rl*, *rIIAB*, and *rIII*, - were
58 foundational in working out the fundamentals of inheritance, the genetic code, mutation,
59 recombination, DNA repair, and gene structure (3-7). These mutable loci were originally
60 discovered by their distinctive plaque morphology: large, clear, sharply-defined plaques,
61 easily distinguished from the small, fuzzy-edged turbid plaques of the parental phages
62 (1). The “*r*” designation meant “rapid lysis”, which refers to the observation that the
63 mutant phages isolated from the r-type plaques caused rapid, culture-wide lysis at ~25
64 min after infection, whereas cultures infected with the parental phages continued to
65 increase in mass and accumulated progeny virions intracellularly for hours, in a state
66 called “lysis inhibition”(LIN)(8). In the ensuing decades, more loci were assigned as *r*
67 genes based on mutant plaque phenotypes; at one point, there were *r* genes numbered
68 up to *rVI* that were assigned map positions (9, 10). In 1998, Paddison *et al.* (11)

69 reviewed this field and concluded that only *rl*, *rIII* and *rV* were directly involved in LIN,
70 with the other genes causing lysis phenotypes through indirect physiological pathways.
71 The *rV* mutants were shown to be missense alleles of gene *t*, which encodes T, the
72 holin of phage T4 (12). Holins are the master lysis control proteins of Caudovirales (13),
73 acting to terminate the infection cycle by permeabilizing the cytoplasmic or inner
74 membrane (IM) at a programmed time. It followed that the simplest operational model to
75 explain the involvement of the remaining loci associated with direct LIN defects, *rl* and
76 *rIII*, would be that the RI and RIII proteins were required to inhibit the lethal function of T
77 and thus establish the LIN state (9, 11).

78 More recent studies on T and RI have confirmed aspects of this operational
79 model for LIN and provided molecular details for the lysis pathway of T4 (14-16). Like
80 other holins, including the well-studied S105 holin of phage lambda, the T holin
81 accumulates harmlessly in the host IM until it suddenly forms lethal, micron-scale
82 membrane lesions at an allele-specific time. This event, which is defined as holin
83 triggering, results in the escape of cytoplasmic endolysin E (product of gene *e*) (13) into
84 the periplasm, where it rapidly degrades the cell wall. In turn, the loss of cell wall
85 activates the spanin complex (product of *pseT.2* and *pseT.3*)(17), which then disrupts
86 the outer membrane (OM) and completes the release of the progeny. In single
87 infections, T4 completes this three-step pathway in ~25 min (1). However, if the T4-
88 infected cells are super-infected by other T4 (or T-even phages) after the first five
89 minutes of the infection cycle, LIN is imposed (18). There has been progress on the
90 molecular basis of LIN (15, 19-21). While most holins have two or more transmembrane
91 domains (TMDs) and only short soluble loops connecting them (13), the T holin has a

92 unique structure, with only a single TMD and significant N- (34 aa) and C-(163 aa)
93 terminal cytoplasmic and periplasmic domains, respectively (15, 22) (**Fig. 1**). Moreover,
94 the RI protein was shown to have a SAR (signal anchor release) domain, which is a
95 TMD that can escape from the membrane (19). By virtue of this domain, RI is secreted
96 initially as a membrane-tethered periplasmic protein and then releases into the
97 periplasm where, in single infections, it is degraded rapidly (19, 20). However, under
98 LIN conditions, (i.e., when there is superinfection with a second T4 phage particle), RI is
99 stabilized and accumulates in the periplasm, where it forms an equimolar complex with
100 the cytoplasmic domain of T and inhibits triggering, thus imposing the LIN state.
101 Additionally, if the SAR domain of RI is replaced by a cleavable Signal Peptidase I
102 signal sequence, the processed RI protein over-accumulates in the periplasm in a
103 stable, mature form, forms the complex with T and imposes LIN without requiring the
104 superinfection activation (19, 20).

105 Because RI is a specific inhibitor of T, it is formally a member of a diverse class
106 of proteins designated as antiholins (23-26). Moreover, since RI inhibits T only under
107 certain physiological conditions, it is the only antiholin known that transduces
108 environmental information to effect real-time control of holin function and thus the length
109 and fecundity of the phage infection cycle (21). However, despite these conceptual and
110 mechanistic advances with T and RI, the genetic basis of the LIN phenomenon remains
111 incomplete, some decades after the genetics of the *r* genes were first published,
112 because no role has been found for *rIII* (1, 3). Although it was reported that RIII was not
113 required for LIN on some K-12 strains (6), *rIII* shares with *rI* the feature that neither
114 locus can suppress *t* lysis-null mutations and both loci are transcribed from both early

115 and late promoters (11, 27). Recently, *rIII* was suggested to play a role in the
116 propagation of T4 in slow-growing host cells (28). Here, we present the preliminary
117 results of *in vivo* and *in vitro* characterization of *rIII*. The results are analyzed in terms of
118 a model that suggests direct molecular involvement of RIII in LIN as a new class of
119 antiholin.

120

121 **Materials and methods**

122 **Bacterial growth and induction**

123 See **Table 1** for the full list of phages and bacteria strains used in this study.
124 Bacterial strains were plated on standard LB-agar plate supplemented with the
125 appropriate antibiotics (ampicillin, 100 $\mu\text{g mL}^{-1}$; chloramphenicol, 10 $\mu\text{g mL}^{-1}$;
126 Kanamycin, 40 $\mu\text{g mL}^{-1}$). A single colony from a LB plate was used to inoculate 3 mL
127 overnight culture at 30°C for λ lysogens and 37°C for non-lysogenic *E. coli* strains, as
128 described before (21). Overnight cultures were diluted to $A_{550} \sim 0.03$ and grown at 30°C
129 or 37°C with aeration. Bacterial growth and lysis were monitored as described (21)
130 using a Gilford Stasar III sipping spectrophotometer (Gilford Instrument Inc, Oberlin,
131 OH). The λ lysogens were induced as described (14, 21). All plasmid-cloned genes
132 were induced with 1 mM isopropyl b-D-thiogalactosidase (IPTG).

133 **Phage infection and preparation of phage lysates**

134 Phage lysates were prepared by adding 10% CHCl_3 (v/v) to the *E. coli* cell culture
135 after lysis, in either induced lysogens or by liquid culture infections, as described
136 previously (19). The lysate was cleared by centrifugation at 5,000 x g and the

137 supernatant was filtered through a 0.22 μm syringe filter. Phage infection experiments
138 were carried out as described (19, 21). For liquid culture infections, host *E. coli* cells
139 were grown to $A_{550} \sim 0.3$ and infected at a multiplicity of infection (MOI) ~ 5 . To observe
140 plaque morphology, 100 μL overnight cultures of host cells were added to 3 mL of LB
141 top agar and immediately poured on standard LB-agar plates. 5 μL of phage lysates
142 with proper dilutions were spotted onto the top agar. For complementation experiment,
143 BL21(DE3) *fhuA::Tn10* cells carrying pET11a vectors were grown to $A_{550} \sim 1$ at 37°C,
144 and induced with 1mM IPTG for 2 h before mixed with LB top agar and poured onto LB
145 plates containing proper antibiotics and 1mM IPTG. All plates were incubated $\sim 16\text{h}$ at
146 37°C. The plaque sizes were analyzed using ImageJ software (NIH, Bethesda, MD).

147 **Standard DNA manipulations and sequencing**

148 All plasmids used in this study are listed in **Table 1**. Isolation of plasmid DNA,
149 DNA amplification by polymerase chain reaction (PCR), DNA transformation, and DNA
150 sequencing were performed as previously described (15, 22, 29). Oligonucleotides
151 (primers) DNA sequences are listed in **Table 2**. All purified oligonucleotides (primers)
152 were purchased from Integrated DNA technologies (Coralville, IA). Restriction and DNA-
153 modifying enzymes were purchased from New England Biolabs (Ipswich, MA).
154 Manufacturer's instructions were followed when performing reactions. The DNA
155 sequence of all constructs was verified by sequencing service provided by Eton
156 Bioscience (San Diego, CA).

157 **PCR and plasmid construction**

158 T4D phage lysate was directly used as the PCR template for cloning out T4
159 genes. Pfu DNA polymerase was used for all PCR reactions following standard

160 protocols provided by Promega (Madison, WI). Site-directed mutagenesis was
161 performed as described (22). The *rIII* gene either with its native ribosome binding site
162 (GAG) or a stronger ribosome binding site (AGGAG) was cloned into the medium-copy
163 IPTG-inducible vector pZE12 (30). Plasmid pZE12-RIII_o and pZE12-RIII_s were
164 constructed by inserting T4 DNA from nt 130738 to nt 131080 (RIII_o), or from nt 130785
165 to nt 131033 (RIII_s) into pZE12 between KpnI and XbaI sites. Plasmid pET11aRIII has
166 the same insertion as pZE12RIII_s between its NdeI and BamHI sites. Plasmid pZE12RI-
167 RIII was made by inserting a tandem clone of *rl* and *rIII* genes with their original
168 ribosome binding site into plasmid pZE12. These plasmids were transformed into a
169 CQ21λ-*t* lysogen, in which the lambda holin gene *S* has been replaced by T4 gene *t*
170 (14). In this system, RI or/and RIII can be expressed *in trans* to T from pZE12 plasmids
171 by adding 1mM IPTG after lysogenic induction. A λS_{A52G} lysogen was used as a control,
172 since the S_{A52G} confers a ~20 min lysis time, similar to the *t* gene (31). Plasmid pTB146
173 is a derivative of plasmid pET11a encoding an N-terminal his6-SUMO tag (29, 32).
174 Plasmids encoding His-SUMO-tagged versions of RIII and nT (the N-terminal domain
175 of T), pTB146-RIII and pTB146-nT were constructed by inserting codon 2-81 of the *rIII*
176 gene, or codons 2-34 of the *t* gene (nt 160218 to nt 160322 of T4 genome),
177 respectively, into the pTB146 plasmid between its SapI and XhoI sites.

178 **Constructing T4 *rIII* deletion mutant**

179 T4Δ*rIII* was constructed by homologous recombination between pZE12-Δ*rIII* and
180 T4D, as described previously for T4Δ*rl* (19). pZE12- Δ*rIII* was made by deleting the *rIII*
181 gene from plasmid pZE12-*rIII*-flank, which contains T4 DNA from nt 130231 to nt
182 131541 between its KpnI and XbaI sites, using our previously described method (33).

183 Plasmid pZE12- $\Delta rIII$ was transformed into *E.coli* strain MDS12 *tonA::Tn10 lacI*^{q1}, and
184 the transformants were grown to $A_{550} \sim 0.4$. The culture was infected with T4D phage at
185 a MOI=10 for 3 h at 37°C with aeration, and then lysed by adding 10% v/v $CHCl_3$. T4 *rIII*
186 recombinants in this lysate were enriched three times for early lysis as described (19).
187 The enriched lysate was plated on *E. coli* B834 and screened for *r* plaque morphology.
188 The $\Delta rIII$ deletion was confirmed by PCR and sequencing.

189 **SDS-PAGE and Western blotting**

190 SDS-PAGE and Western blotting were conducted as previously described (22)
191 10% trichloroacetic acid (TCA) was used to precipitate proteins from the whole-cell
192 samples. Reducing sample loading buffer (SLB) supplemented with β -mercaptoethanol
193 was used for resuspending protein samples unless otherwise indicated. RIII proteins
194 transferred onto PVDF membrane were detected using rabbit polyclonal anti-RIII (α -
195 RIII) antibody purchased from Genscript (Piscataway, NJ). The monoclonal anti-his-tag
196 antibody (α -his) was purchased from Sigma-Aldrich (Carlsbad, CA). To detect proteins,
197 blots were incubated overnight at 4°C with α -RIII or α -his at a dilution of 1:4000 in 3%
198 milk-TBS buffer. Blots were developed with the West Femto SuperSignal
199 Chemiluminescence kit purchased from Thermo Fisher Scientific (Rockford, IL). The
200 chemiluminescence signal was detected using a Bio-Rad Chemidoc XRS (Bio-Rad
201 Laboratories, Hercules, CA). Images were obtained and analyzed by Quantity One 1-D
202 Analysis Software (Bio-Rad Laboratories, Philadelphia, PA).

203

204

205

206 **Bacterial two hybrid assay**

207 Bacterial two hybrid (B2H) assays were conducted as described previously (34-
208 36). Plasmids were constructed by inserting codons 2-81 of the *rIII* gene, or codons 2-
209 34 of the *t* gene into plasmids pCH363, pKNT25, pCH364, and pKT25, as described
210 (36). Different pairs of plasmid were transformed into strain DHP1 and grown to $A_{550} \sim$
211 0.3 in LB with 0.2% glucose and appropriate antibiotics (ampicillin, 50 $\mu\text{g mL}^{-1}$;
212 kanamycin, 25 $\mu\text{g mL}^{-1}$). For the plate assay, 5 μL of cell cultures were spotted on M9
213 minimal media plates supplemented with 0.2% glucose, 40 $\mu\text{g mL}^{-1}$ X-Gal, 150 μM
214 IPTG and proper antibiotics and incubated for 48h at 25°C.

215 **Pull-down assays**

216 Plasmid pET11a and pTB146 derivatives described above were transformed into
217 BL21(DE3) *fhuA::Tn10* strains. Pull-down assays were conducted as instructed by
218 manufacturer protocol from Dynabeads® His-Tag Isolation and Pulldown kit (Thermo
219 Fisher Scientific, Rockford, IL). All incubation and reaction were carried out in 4°C and
220 beads were collected using DynaMag™-2 Magnet (Thermo Fisher Scientific). All
221 samples were resuspended in SLB and boiled for 5 min to elute proteins, which were
222 then analyzed by SDS-PAGE and Western blotting, which were performed as described
223 above.

224

225 **Results**226 ***rIII* is required for LIN in both *E. coli* B and K-12 background**

227 The role of *rIII* in LIN has been ambiguous, with reports differing in whether *rIII*
228 was required on *E. coli* B but not K-12 strains (6, 9, 37). In our hands, the classic *rIII*
229 allele T4r67, which was used as the standard allele in the early T4 genetic map studies,
230 formed r-type plaques on the lawns of both *E. coli* B834 and MG1655 (**Fig. 2A**), with
231 somewhat smaller plaques compared to those formed by T4rI, but significantly larger
232 than wt T4 plaques (**Table 3**). It was also reported that different T4 *rIII* mutants differed
233 in plaque size, suggesting a possible correlation between the location of mutations on
234 *rIII* locus and plaque morphology (38). However, when we compared plaque
235 morphologies of four different T4 *rIII* defective mutants (T4r67, T4rBB9, T4rES35, and
236 T4rES40) on B834, we did not observe significant differences (**Table 3**). Nevertheless,
237 as the first step for interrogating the role of *rIII* in LIN, we constructed an *rIII* deletion
238 allele, T4Δ*rIII*, to eliminate the potential for partial reversion. As shown in **Table 3** and
239 **Fig. 2A**, T4Δ*rIII* formed r-type plaques that were larger than wt plaques, but smaller
240 than those of T4rI. Moreover, the wt plaque morphology could be complemented by a
241 plasmid-borne *rIII* gene (**Fig. 2B**). In infections of both *E. coli* B or K-12 cultures under
242 conditions where the wt T4 exhibited LIN, T4Δ*rIII* infections showed lysis at ~25 min, in
243 both cases reproducibly later than the lysis time of T4Δ*rI* (~18 min), (**Fig. 3A**). The
244 simplest notion, based on the established role of RI in LIN, is that RI expressed in the
245 T4Δ*rIII* infection causes transient LIN, and that, by extension, RIII is required for stable
246 LIN in both *E. coli* B and K-12 strains.

247

248 Identification of the RIII protein

249 *rIII* encodes an 82aa polypeptide without any secretion signals (Fig. 4A) and had
250 not been identified as a protein species in T4-infected cultures. We raised a polyclonal
251 antibody against an RIII oligopeptide sequence predicted to be highly immunogenic
252 (Fig. 4A). The RIII protein could be visualized by immunoblotting in samples taken from
253 cells infected with T4wt, but not with T4 Δ *rIII* (Fig. 4B); the mobility of this RIII species
254 corresponded to a slightly lower molecular mass than predicted (8.9 kDa versus 9.3 kDa
255 predicted), presumably due to the high content of charged residues (24 out of 82) (Fig.
256 4A).

257 Recapitulating the role of RIII in LIN in the λ context

258 To address the role of RIII in LIN, we used a convenient system based on the
259 inducible lambda prophage, λ -t, in which the λ holin gene S is replaced by T4 *t* (14). Not
260 only was this hybrid phage previously shown to recapitulate T4 lysis timing and LIN at
261 physiological levels of expression, it allows the co-expression of selected T4 genes
262 cloned in inducible plasmid vectors without the confounding effects of T4-mediated host
263 DNA degradation and translational repression(14, 15, 21, 39). This system mimics the
264 T-dependent lysis in the λ context where effects of T4 genes other than *t* are excluded.
265 To provide RIII in trans, the *rIII* gene was cloned into a medium copy-number plasmid
266 vector pZE12 (30). Two isogenic clones were constructed with different Shine-Dalgarno
267 (SD) sequences serving the *rIII* cistron, one the relatively weak native sequence (GAG)
268 and the other with a stronger near-consensus sequence (AGGAG). The resulting
269 plasmids pZE12RIII_o (original SD sequence) and pZE12RIII_s (strong SD sequence)
270 were transformed into the λ -t lysogen. Induction of the λ -t lysogen resulted in

271 reproducible and sharply defined lysis at ~ 20 min; induction of pZE12RIII_s with IPTG
272 conferred a mild but reproducible lysis delay of ~5 min (**Fig. 3B**). In contrast, lysis was
273 much more severely affected by induction of an isogenic clone of the T4 antiholin gene
274 *rl*, as previously shown (21). Induction of pZE12RIII_o did not affect the lysis timing,
275 probably due to the lower protein expression level (Data not shown).

276 We next asked if RIII can extend RI-mediated LIN. An isogenic plasmid with *rl*
277 and *rIII* cloned in tandem was constructed and introduced into the λ -*t* lysogen. Induction
278 of this plasmid, pZE12RI-RIII, led to a drastically delayed LIN compared to induction of
279 either pZE12RIII_s or pZE12RI (**Fig. 3B**); under these conditions, the LIN state lasted up
280 to 80 min and then gradually deteriorated. Using this system, we tested three *rIII*
281 missense alleles isolated by UV mutagenesis: G24D, H42R, and A70V (9) (**Fig. 4A**). In
282 the absence of RI, two of the alleles, G24D and H42R, exhibited a slight but
283 reproducible LIN defect, although the phenotype was subtle due to the relatively small
284 effect of the parental *rIII* allele under these conditions (**Fig. 3C**). Co-induction of these
285 *rIII* with *rl*, however, resulted in distinct intermediate LIN defects, with lysis times ranging
286 from 40 min~60 min, indicating these are partially defective alleles, at least in the
287 lambda context (**Fig. 3C**). The lysis blockage was *t*-specific, as indicated by the fact that
288 isogenic experiments with a lambda holin allele, *S*_{A52G}, which has an early lysis
289 phenotype that matches the normal *t* lysis time (31), did not show lysis delays in
290 inductions of pZE12RIII_s, pZE12RI or pZE12RI-RIII (**Fig. 3B**). Taken together, these
291 data indicated that RIII has T-specific antiholin activity.

292 **RIII binds to the cytoplasmic N-terminus of T**

293 Next we addressed the molecular basis of RIII participation in LIN. The simplest
294 hypothesis is, like other antiholins, including RI, RIII affects holin triggering by directly
295 binding to holin T and blocking hole formation in the IM. Since RIII has no membrane or
296 export signals (**Fig. 4A**), the only possible target for RIII is the N-terminal cytoplasmic
297 domain of T (nT), which has 34aa, and is required for holin function (15). To test this
298 idea, we used the bacterial two hybrid system, based on intragenic complementation of
299 CyaA function (34). We fused the nT, wt RIII, and four RIII mutant allele sequences to
300 various combinations of the T25 and T18 fragments of CyaA. As shown in **Fig. 5A**, this
301 system revealed a strong self-interaction of RIII *in vivo*, which was abolished in the
302 G24D allele, partially affected by H42R, and unaffected by L43Q or R75C. The
303 transformants carrying plasmids expressing T18-RIII and T25-nT resulted in light but
304 reproducible signals (**Fig. 5B**), suggesting a relatively weak interaction between RIII and
305 nT. Significantly, none of the four RIII mutant fusions retained the nT-binding ability
306 (**Fig. 5B**). These results correlate with the liquid culture lysis results (**Fig. 3C**) and
307 indicate the nT-RIII interaction is affected by the changes in the lysis-defective RIII
308 alleles.

309 To address the nT-RIII interaction *in vitro*, we constructed versions of nT and RIII
310 tagged at the N-terminus with the His6-Sumo moiety (See Materials and Methods). After
311 induction in a T7-based over-expression system, both His6-Sumo-nT and His6-Sumo-
312 RIII accumulated as soluble forms (**Fig. 6, top panel, lanes 2-5**). To detect complexes
313 formed *in vitro*, the SUMO-tagged nT and RIII proteins were bound to magnetic beads,
314 mixed with cell lysates containing wt RIII or mutant RIII_{H42R} protein, fractionated as

315 bound and unbound, and then analyzed by immunoblotting. The results showed that
316 both wt RIII and mutant RIII_{H42R} proteins form complexes with His6-Sumo-RIII, but only
317 wt RIII complexes with His6-Sumo-nT (**Fig. 6, bottom panel**). The simplest
318 interpretation is that the H42R mutation completely abrogates the RIII-nT interface but
319 not the RIII homo-oligomerization interface, which is consistent with the results of the
320 bacterial two-hybrid experiments.

321 **The cytoplasmic N-terminal domain of T can block lysis inhibition in an RIII-** 322 **specific manner**

323 The finding that RIII binds nT in vitro and in *E. coli* in the context of the two-
324 hybrids suggested that the *r* phenotype could be imposed in vivo by titrating the RIII
325 produced in a T4 infection with the Sumo-tagged nT derivative. To test this idea, we
326 plated T4 on lawns of cells induced for the over-expression of His6-Sumo-nT; under
327 these conditions, T4 wt generated plaques distinctly larger and cleared compared to
328 those generated on the isogenic control strain expressing the His6-Sumo tag (**Fig. 7**).
329 Neither T4*rIII* nor T4 Δ *rIII* plaque morphology was affected by overexpression of nT (**Fig**
330 **7**).

331 **Discussion**

332 Among the Caudovirales, the lysis timing effected by the holin defines the length
333 and fecundity of the phage infection cycle. Mutational analysis has shown that holin-
334 mediated lysis timing can be drastically altered by single missense changes (15, 39-41),
335 leading to the suggestion that this extreme mutational sensitivity is an evolutionary
336 fitness factor, allowing phages to mutate rapidly to a radically different length of life

337 cycle in response to altered environmental conditions (42). Despite the implied
338 correlation between lysis timing and the environment, the T4 LIN phenomenon remains
339 the only documented example of real-time regulation of lysis timing. Genetic analysis
340 has shown that mutations in two of the classic T4 plaque-morphology loci, *rl* and *rV*, the
341 latter allelic to the *t* holin gene, confer an absolute defect in LIN. Our work had shown
342 that RI is a secreted protein that is initially synthesized as periplasmic protein tethered
343 to the membrane with an N-terminal signal-anchor-release (SAR) domain (19). The
344 presence of the SAR domain allows it to release into the periplasm and also confers
345 extreme proteolytic instability on RI. Over-expression of the wt *rl* gene was shown to
346 impose a delay on T-holin triggering in the lambda context. A chimeric *rl* gene in which
347 the SAR domain was replaced by a cleavable signal sequence generated a
348 proteolytically stable periplasmic RI and, expressed in trans to *t*, imposed a stable LIN
349 state. A model has been proposed in which an unknown LIN signal is generated by a
350 super-infecting T4 virion. Under these conditions, it is suggested that the T4 Spackle
351 and Imm proteins force the superinfecting virion to eject its capsid contents ectopically
352 into the host periplasm (43). Some component of these virion contents, which include
353 both the T4 genomic DNA and ~1000 protein molecules (11, 37), acts as a signal to
354 stabilize the periplasmic RI protein. In this model, RI accumulates and binds to the
355 periplasmic domain of the T4 holin T in a manner that T triggering is inhibited.(19).
356 Significant progress has been made on the RI-T interaction. The soluble domain of RI,
357 sRI, has been purified and shown to be largely alpha-helical in structure (22). In
358 addition, the sRI molecule was able to bind the soluble domain of T, sT (22, 44), and
359 prevent it from aggregation. Crystal structures of sRI and the sRI:sT complex have been

360 determined (44). However, major gaps remained in our understanding of the LIN
361 phenomenon. First of all, the signal provided by the superinfecting phage is completely
362 unknown. In addition, the possible role of other *r* loci, most notably *rIII*, was not reflected
363 in the model.

364 In this study we have shown that *rIII* is also unambiguously required for LIN on
365 both *E. coli* K-12 and B hosts, resolving a long-standing controversy (9, 11). Moreover,
366 we have shown the *rIII* gene expressed *in trans* to the T4 holin gene *t* can effect a small
367 but reproducible lysis delay in a T-specific manner. In addition, expression of *rIII*
368 significantly stabilized the LIN state imposed by over-expression of wt *rl*, which
369 otherwise imposes a lysis delay that collapses after ~45 min. Since RIII is a cytoplasmic
370 protein, the simplest notion is that RIII acts by binding to the short cytoplasmic domain
371 of T, nT. Evidence supporting this was obtained from bacterial two-hybrid analysis and
372 pull-down assays, which revealed a specific interaction between nT and the full-length
373 RIII polypeptide. Importantly, known dysfunctional *rIII* missense mutations caused a
374 defect in the RIII-mediated stabilization of RI-LIN. Finally, bacterial two-hybrid evidence
375 was provided showing that RIII has dimerizing or oligomerizing propensity, which may
376 be functionally important in view of the fact that one of the known *rIII* defective missense
377 mutations abrogates the response.

378 Taken together, these results indicate that both RI and RIII are, strictly defined,
379 specific antiholins of the T4 holin T, and suggest an expansion of our previous model to
380 include inhibitory interactions on both sides of the cytoplasmic membrane (**Fig. 8**). In
381 this scenario, RI acts as the LIN master regulator by receiving the signal generated by
382 the super-infecting virion. Stabilization of RI leads to the formation of RI-T complexes

383 that prevent the T protein from participating in the holin triggering pathway. The
384 available evidence indicates that holin triggering occurs when the holin reaches a critical
385 two-dimensional concentration and forms large oligomers, or rafts, within which the
386 lethal holes are formed (42, 45). The simplest notion is that RI may simply block homo-
387 oligomerization of T and thus T-triggering, which is consistent with the ability of sRI to
388 prevent aggregation of sT (20). In our new model, we suggest that RIII participates in
389 LIN by stabilizing the RI-T complexes. Indeed, the sRI:sT crystal structures were in the
390 form of sT:sRI:sRI:sT hetero-tetramers (44). Thus an attractive notion is that in the
391 onset of LIN, T-RI-RI-T heterotetramers are formed providing a symmetric binding site
392 for RIII dimers to bind to the cytoplasmic nT domains (**Fig. 8**). It should be noted that, in
393 this perspective, RIII is the first example of an antiholin with no secretory or membrane
394 signal, and also that the RI-RIII combination is the first example of a multiple-antiholin
395 system. Since stabilizing RI by removal of the SAR domain can lead to stable LIN
396 without the participation of RIII, we propose to designate RI as the antiholin with RIII as
397 a co-antiholin.

398 As noted above, major gaps remain in our understanding of the T4 LIN
399 phenomenon, which deserves attention not only because of its historical status, but as a
400 richly-documented phenomenon that may be important in our understanding of phage
401 propagation in liquid culture and in environmental scenarios that may be relevant to
402 phage-based therapeutics. Immediate future efforts will be directed at determining the
403 nature of the RIII-nT interaction at the structural level.

404

405 **Acknowledgement**

406 This research was supported by Public Health Service grant GM27099 to R.Y.
407 and by funding from the Center for Phage Technology (CPT). The CPT is jointly
408 supported by Texas A&M University and Texas A&M AgriLife Research. We thank Yi
409 Duan and Allyssa Miller from the Herman laboratory for providing plasmids, strains, and
410 advice for implementation of the bacterial two-hybrid assay. We also thank the Young
411 laboratory and Center for Phage Technology members, past and present, for their
412 helpful discussion, criticisms and suggestions.

413

414

415

416

417

418

419

420

421

422

423

424

425

426

427

428 **Literature cited or References:**

- 429 1. **Hershey AD.** 1946. Mutation of Bacteriophage with Respect to Type of Plaque.
430 Genetics **31**:620-640.
- 431 2. **Doermann AH.** 1948. Lysis and Lysis Inhibition with Escherichia coli
432 Bacteriophage. J Bacteriol **55**:257-276.
- 433 3. **Hershey AD, Chase M.** 1951. Genetic recombination and heterozygosis in
434 bacteriophage. Cold Spring Harb Symp Quant Biol **16**:471-479.
- 435 4. **Benzer S.** 1955. Fine Structure of a Genetic Region in Bacteriophage. Proc Natl
436 Acad Sci U S A **41**:344-354.
- 437 5. **Crick FH, Barnett L, Brenner S, Watts-Tobin RJ.** 1961. General nature of the
438 genetic code for proteins. Nature **192**:1227-1232.
- 439 6. **Benzer S.** 1957. The Elementary Units of Heredity. In WILLIAM D. McELROY
440 BG (ed.), The Chemical Basis of Heredity. Johns Hopkins University Press,
441 Baltimore.
- 442 7. **Hershey AD, Rotman R.** 1948. Linkage Among Genes Controlling Inhibition of
443 Lysis in a Bacterial Virus. Proc Natl Acad Sci U S A **34**:89-96.
- 444 8. **Hershey AD.** 1946. Spontaneous mutations in bacterial viruses, Cold Spring
445 Harb Symp Quant Biol, vol. 11: 67-77. Cold Spring Harbor Laboratory Press.
- 446 9. **Burch LH, Zhang L, Chao FG, Xu H, Drake JW.** 2011. The bacteriophage T4
447 rapid-lysis genes and their mutational proclivities. J Bacteriol **193**:3537-3545.
- 448 10. **Krylov VN, Yankovsky NK.** 1975. Mutations in the new gene still of
449 bacteriophage T4B suppressing the lysis defect of gene still and a gene e mutant.
450 J Virol **15**:22-26.
- 451 11. **Paddison P, Abedon ST, Dressman HK, Gailbreath K, Tracy J, Mosser E,**
452 **Neitzel J, Guttman B, Kutter E.** 1998. The roles of the bacteriophage T4 r
453 genes in lysis inhibition and fine-structure genetics: a new perspective. Genetics
454 **148**:1539-1550.
- 455 12. **Dressman HK, Drake JW.** 1999. Lysis and lysis inhibition in bacteriophage T4:
456 rV mutations reside in the holin t gene. J Bacteriol **181**:4391-4396.
- 457 13. **Young R.** 1992. Bacteriophage lysis: mechanism and regulation. Microbiol Rev
458 **56**:430-481.
- 459 14. **Ramanculov E, Young R.** 2001. Functional analysis of the phage T4 holin in a
460 lambda context. Mol Genet Genomics **265**:345-353.
- 461 15. **Moussa SH, Lawler JL, Young R.** 2014. Genetic dissection of T4 lysis. J
462 Bacteriol **196**:2201-2209.
- 463 16. **Josslin R.** 1970. The lysis mechanism of phage T4: mutants affecting lysis.
464 Virology **40**:719-726.
- 465 17. **Summer EJ, Berry J, Tran TA, Niu L, Struck DK, Young R.** 2007. Rz/Rz1 lysis
466 gene equivalents in phages of Gram-negative hosts. J Mol Biol **373**:1098-1112.
- 467 18. **Bode W.** 1967. Lysis inhibition in Escherichia coli infected with bacteriophage
468 T4. J Virol **1**:948-955.
- 469 19. **Tran TA, Struck DK, Young R.** 2007. The T4 RI antiholin has an N-terminal
470 signal anchor release domain that targets it for degradation by DegP. J Bacteriol
471 **189**:7618-7625.

- 472 20. **Tran TA, Struck DK, Young R.** 2005. Periplasmic domains define holin-antiholin
473 interactions in t4 lysis inhibition. *J Bacteriol* **187**:6631-6640.
- 474 21. **Ramanculov E, Young R.** 2001. An ancient player unmasked: T4 rl encodes a t-
475 specific antiholin. *Mol Microbiol* **41**:575-583.
- 476 22. **Moussa SH, Kuznetsov V, Tran TA, Sacchettini JC, Young R.** 2012. Protein
477 determinants of phage T4 lysis inhibition. *Protein Sci* **21**:571-582.
- 478 23. **Blasi U, Chang CY, Zagotta MT, Nam KB, Young R.** 1990. The lethal lambda S
479 gene encodes its own inhibitor. *EMBO J* **9**:981-989.
- 480 24. **White R, Tran TA, Dankenbring CA, Deaton J, Young R.** 2010. The N-terminal
481 transmembrane domain of lambda S is required for holin but not antiholin
482 function. *J Bacteriol* **192**:725-733.
- 483 25. **To KH, Dewey J, Weaver J, Park T, Young R.** 2013. Functional analysis of a
484 class I holin, P2 Y. *J Bacteriol* **195**:1346-1355.
- 485 26. **Barenboim M, Chang CY, dib Hajj F, Young R.** 1999. Characterization of the
486 dual start motif of a class II holin gene. *Mol Microbiol* **32**:715-727.
- 487 27. **Luke K, Radek A, Liu X, Campbell J, Uzan M, Haselkorn R, Kogan Y.** 2002.
488 Microarray analysis of gene expression during bacteriophage T4 infection.
489 *Virology* **299**:182-191.
- 490 28. **Golec P, Karczewska-Golec J, Voigt B, Albrecht D, Schweder T, Hecker M,
491 Wegrzyn G, Los M.** 2013. Proteomic profiles and kinetics of development of
492 bacteriophage T4 and its rl and rIII mutants in slowly growing *Escherichia coli*. *J*
493 *Gen Virol* **94**:896-905.
- 494 29. **Berry J, Savva C, Holzenburg A, Young R.** 2010. The lambda spanin
495 components Rz and Rz1 undergo tertiary and quaternary rearrangements upon
496 complex formation. *Protein Sci* **19**:1967-1977.
- 497 30. **Lutz R, Bujard H.** 1997. Independent and tight regulation of transcriptional units
498 in *Escherichia coli* via the LacR/O, the TetR/O and AraC/I1-I2 regulatory
499 elements. *Nucleic Acids Res* **25**:1203-1210.
- 500 31. **Johnson-Boaz R, Chang CY, Young R.** 1994. A dominant mutation in the
501 bacteriophage lambda S gene causes premature lysis and an absolute defective
502 plating phenotype. *Mol Microbiol* **13**:495-504.
- 503 32. **Bendezu FO, Hale CA, Bernhardt TG, de Boer PA.** 2009. RodZ (YfgA) is
504 required for proper assembly of the MreB actin cytoskeleton and cell shape in *E.*
505 *coli*. *EMBO J* **28**:193-204.
- 506 33. **Hansson MD, Rzeznicka K, Rosenback M, Hansson M, Sirijovski N.** 2008.
507 PCR-mediated deletion of plasmid DNA. *Anal Biochem* **375**:373-375.
- 508 34. **Karimova G, Pidoux J, Ullmann A, Ladant D.** 1998. A bacterial two-hybrid
509 system based on a reconstituted signal transduction pathway. *Proc Natl Acad Sci*
510 *U S A* **95**:5752-5756.
- 511 35. **Battesti A, Bouveret E.** 2012. The bacterial two-hybrid system based on
512 adenylate cyclase reconstitution in *Escherichia coli*. *Methods* **58**:325-334.
- 513 36. **Miller AK, Brown EE, Mercado BT, Herman JK.** 2016. A DNA-binding protein
514 defines the precise region of chromosome capture during *Bacillus* sporulation.
515 *Mol Microbiol* **99**:111-122.
- 516 37. **Christopher K. Mathews EMK, Gisela Mosig, Peter B. Berget.** 1983.
517 Bacteriophage T4. American Society of Microbiology, Washington, D.C.

- 518 38. **Raudonikiene A, Nivinskas R.** 1992. Gene rIII is the nearest downstream
519 neighbour of bacteriophage T4 gene 31. *Gene* **114**:85-90.
- 520 39. **Ramanculov E, Young R.** 2001. Genetic analysis of the T4 holin: timing and
521 topology. *Gene* **265**:25-36.
- 522 40. **Pang T, Park T, Young R.** 2010. Mutational analysis of the S21 pinholin. *Mol*
523 *Microbiol* **76**:68-77.
- 524 41. **Raab R, Neal G, Garrett J, Grimaila R, Fusselman R, Young R.** 1986.
525 Mutational analysis of bacteriophage lambda lysis gene S. *J Bacteriol* **167**:1035-
526 1042.
- 527 42. **Young R.** 2013. Phage lysis: do we have the hole story yet? *Curr Opin Microbiol*
528 **16**:790-797.
- 529 43. **Obringer JW.** 1988. The functions of the phage T4 immunity and spackle genes
530 in genetic exclusion. *Genet Res* **52**:81-90.
- 531 44. **Kuznetsov VB.** 2011. Structural Studies of Phage Lysis Proteins and Their
532 Targets. Doctoral dissertation, Texas A&M University, College Station.
- 533 45. **To KH, Young R.** 2014. Probing the structure of the S105 hole. *J Bacteriol*
534 **196**:3683-3689.

535

536

537

538

539

540

541

542

543

544

545

546

547

548

549

550

551

552 **Figure Legends**

553 **FIG 1** Topology of T4 holin T -antiholin RI interaction. T is an inner membrane protein
554 with a single TMD (shown as a solid cylinder) and an amphipathic helix (shown as a
555 white cylinder). RI has a SAR (Signal Anchor-Release) domain (shown as a dash line
556 rectangle) which allows RI to be spontaneously released in to the periplasm (19). If
557 stabilized by the LIN signal, periplasmic RI binds to the C-terminal globular periplasmic
558 domain of T. IM, inner membrane.

559 **FIG 2** Plaque morphologies of T4 and its *r* mutants. **(A)** Plaque morphology of T4 wt
560 (T4D) and T4 mutants on either *E. coli* B strain (B834) or *E. coli* K-12 strain (MG1655).
561 The black bar represents 2.5mm. Average plaque sizes of T4D, T4 $\Delta rIII$, T4 $rIII$ and T4 ΔrI
562 on *E. coli* B834 or *E. coli* MG1655 are listed in Table 3. **(B and C)** Complementation of
563 *r* plaque morphology. T4 *rIII* mutants plated on *E. coli* strains expressing wt RIII restored
564 wt T4 plaque morphology, whereas the expression of RIIIH42R did not. In B, differences
565 in plaque sizes were shown as the ratio of the average phage plaque radius (*r*) to the
566 average plaque radius of T4D plated on B834 (r_0). 1, MG1655; 2, BL21(DE3)
567 *fhuA::Tn10* no plasmid; 3, BL21(DE3) *fhuA::Tn10* pET11a pET11a-RIII; 4, BL21(DE3)
568 *fhuA::Tn10* pET11a-RIII_{H42R}.

569 **FIG 3 (A)** Lysis in infections of T4 and derivatives infecting *E. coli* B strain B834 (Left,
570 solid line) or K-12 strain MG1655 (right, dotted line). ×, no phage; ●, T4D (wt); ▲,
571 T4 ΔrI ; △, T4 $\Delta rIII$. Cultures were grown to $A_{550} \sim 0.25$ at 37°C, then infected with T4 at
572 MOI~5. **(B)** Inductions (at t=0) of CQ21 λ -t (Left, solid symbols) or CQ21 λ S_{A52G} (right,
573 open symbols) lysogens carrying indicated genes cloned under IPTG control in the

574 context of the pZE12 plasmid. Plasmids were also induced by addition of 1mM IPTG at
575 $t=0$. ×, luc (negative control); ▲ and △, RI; ● and ○, RIII; ◆ and ◇, RI-RIII. (C) RIII
576 missense mutants exhibit intermediate LIN phenotype. CQ21λ-t lysogens carrying
577 pZE12 plasmids with indicated genes were induced at $t=0$. ×, luc; ▲, RI; ●, RIII; ◆,
578 RI-RIII. Left pane with dotted lines: □, RIII_{G24D}; ◇, RIII_{H42R}; ▽, RIII_{A70V}. Right panel with
579 solid lines: □, RI-RIII_{G24D}; ◇, RI-RIII_{H42R}; ▽, RI-RIII_{A70V}.

580 **FIG 4 (A)** Primary structure of RIII and N-terminus of T4 holin T (nT) with LIN-defective
581 and lysis-defective alleles indicated by black arrows. Conserved residues are
582 underlined. The shaded area represents the oligopeptide used to raise the anti-RIII
583 antibody. Predicted secondary structure is indicated: white box, helix; solid line, turn;
584 white arrow, beta-sheet; grey box, amphipathic helix. (B) RIII protein accumulates
585 during infection. For each sample, 1 A600 equivalent of cells was loaded. The anti-RIII
586 antibody was used in Western blotting. Black arrow indicates predicted molecular mass
587 (9.3kDa) for RIII monomer.

588 **FIG 5** Bacterial two-hybrid results showing self-interaction of RIII (A) and interaction of
589 RIII and N-terminus of T (nT) (B). T18, protein fused to T18 fragment of CyaA protein;
590 T25, protein fused to T25 fragment of CyaA. Negative control (--) indicates T18 or T25
591 fragments without RIII or nT fusion.

592 **FIG 6** *In vitro* interaction between nT and RIII. His-Sumo-tagged nT or RIII was bound
593 to anti-his Dynabeads, and RIII protein pulled down by Dynabeads was analyzed by
594 Western blotting. His-sumo tag only (lane 1, dash black arrow), His-sumo nT (lane 2

595 and 4, black arrow head), His-sumo RIII (lane 3 and 5, white arrow) are shown in the
596 upper panel as the result of western blotting using anti-his antibody. RIII protein (solid
597 black arrow) is visualized in the bottom panel using anti-RIII antibody.

598 **FIG 7** Rescue of *r* plaque morphology by overexpression of the N-terminus of T (nT).
599 **(A)** T4 phages were plated on lawns of *E. coli* BL21(DE3) *fhuA::Tn10* carrying control
600 plasmid expressing His-sumo-nT (pTB146-nT, bottom panels) or His-sumo (pTB146,
601 top panels, neg control). Black bar represents 2.5mm. **(B)** Quantification of plaque sizes
602 were shown as the ratio of the average plaque radius (*r*) to the ratio of T4D plaques
603 plated on pTB146 (*r*₀). Black bar, T4D; Patterned bar, T4Δ*r*III; White bar, T4*r*III.

604 **FIG 8** The current model of LIN involving two antiholins. Both RI and RIII are required
605 for the stable LIN. **(A)** In a single phage infection, antiholin RI will be degraded by
606 periplasmic protease DegP after spontaneous release into the periplasm. Cell lysis
607 occurs at ~ 25 min. **(B)** In a superinfection, the DNA of a superinfecting T4 phage will be
608 ectopically ejected into the periplasm, generating the “signal” to stabilize the periplasmic
609 antiholin RI. This leads to accumulation of RI, which then binds the periplasmic domain
610 of T, in a T-RI-RI-T heterotetramer. This facilitates the binding of cytoplasmic antiholin
611 RIII to the N-terminus of T. This unique, sandwich-like structure spanning two cell
612 compartments robustly blocks participation of T in hole-formation.

613

614

615

616 **TABLE 1** Phages, strains, and plasmids used in this study.

Phages	Description	Source
T4wt	Bacteriophage T4D	Laboratory Stock
T4 <i>rIII</i>	T4 <i>r67</i> . H42 to R (CAU to CGU) mutation in <i>rIII</i> locus.	Laboratory Stock
T4Δ <i>rl</i>	Complete deletion of <i>rl</i> from nt 59204 to nt 59496 in T4D genome	(19)
T4Δ <i>rIII</i>	Complete deletion of <i>rIII</i> from nt 130779 to nt 131042 in T4D genome	This study
λ-t	λ with holin gene <i>S</i> replaced with T4 holin gene <i>t</i>	(14)
λ <i>S</i> _{A52G}	λ <i>cl857</i> carrying Ala52Gly early lysis allele of <i>S</i> holin gene.	(31)
T4 <i>rBB9</i>	W16 to stop (UGG to UGA) mutation in <i>rIII</i> locus	Laboratory Stock
T4 <i>rES35</i>	H42 to Q (CAU to CAA) mutation in <i>rIII</i> locus	Laboratory Stock
T4 <i>rES40</i>	K82 to E (AAG to GAG) mutation in <i>rIII</i> locus	Laboratory Stock
Bacteria Strains	Description	Source
CQ21	<i>E. coli</i> K-12 <i>ara leu lacI^{q1} purE gal his argG rpsL xul mtl ilv</i>	Laboratory Stock
CQ21 λ-t	CQ21 lysogen carrying λ-t prophage	(14)
CQ21 λ <i>S</i> _{A52G}	CQ21 lysogen carrying λ <i>SA52G</i> prophage	This study
BL21(DE3) <i>fhuA::Tn10</i>	<i>E. coli</i> B <i>ompT r_B⁻ m_B⁻ (P_{lac}UV5::T7 gene1) slyD::Kan fhuA::Tn10</i>	Laboratory Stock
B834	<i>E. coli</i> B <i>ompT r_B⁻ m_B⁻ met⁻</i>	Laboratory Stock
MG1655	<i>E. coli</i> F- <i>lambda- ilvG- rfb-50 rph-1</i>	Laboratory Stock
MDS12 <i>tonA::Tn10</i> <i>lacI^{q1}</i>	MG1655 with 12 deletions, totaling 376,180 nt including cryptic prophages	(19)
DHP1	<i>E. coli</i> F- <i>cya-99 araD139 galE15, galK16, rpsL1 (Strr) hsdR2 mcrA1 mcrB1</i>	(36)
Plasmids	Description	Source
pZE12	ColE1 origin; P _{LlacO-1} (PL promoter with three lacO	(30)

	operators); AmpR	
pZE12-luc	Luciferase gene luc cloned under P _{LlacO-1}	(30)
pZE12RI	T4 <i>rl</i> cloned under P _{LlacO-1} with native SD	(21)
pZE12RIII _o	T4 <i>rIII</i> cloned under P _{LlacO-1} with native SD	(21)
pZE12RIII _s	T4 <i>rIII</i> cloned under P _{LlacO-1} with plasmid SD	This study
pZE12RI-RIII	Tandem clone of <i>rl- rIII</i> inserted between KpnI and XbaI site	This study
pET11a-RIII	pBR322 origin, T7 promoter, carrying codon 1-82 of <i>rIII</i>	This study
pET11a-RIII _{H42R}	H42 to R (CAU to CGU) mutation in <i>rIII</i>	This study
pTB146	<i>bla lacI^q</i> PT7::h-sumo	(32)
pTB146-RIII	Codon 2-82 of <i>rIII</i> gene inserted between SapI and XhoI site	This study
pTB146-nT	Codon 2-34 of <i>t</i> gene inserted between SapI and XhoI site	This study
pCH364	T18-empty (AmpR); N-terminal tag	(36)
pKNT25	Empty-T25 (KanR); C-terminal tag	(35, 36)
pKT25	T25-empty (KanR); N-terminal tag	(35, 36)
pCH364RIII	Codon 2-82 of <i>rIII</i> gene inserted between BamHI and EcoRI site	This study
pKNT25RIII	Codon 2-82 of <i>rIII</i> gene inserted between XbaI and EcoRI site	This study
pKT25nT	Codon 2-34 of <i>t</i> gene inserted between BamHI and EcoRI site	This study

TABLE 2 List of oligonucleotides (primers)

Primer name	Sequence	Source
RIII _s CLONING F	CGGTACATTAAACAATTACAACACGCTC	This study
RIII _s CLONING R	GGCTCTAGATTACTTCAGTGTTACCACAAAAGTG	This study
RIII _s PET F	GGAATTCCATATGATTAAACAATTACAACACGCTC	This study
RIII _s PET R	GCGGGATCCTTACTTCAGTGTTACCACAAAAGTG	This study
RIII DEL +500 F	GGGGTACCCATCTGTTAACAAAAAGGAAAAACG	This study
RIII DEL -500 R	GCTCTAGAGCGTTCAGATTAATCGTTTTC	This study
RIII DEL MIX F	TTTTAATCTCTAACGAGGGAGATTCCTGCCT TAGTGTGAGC	This study
RIII DEL MIX R	CCGAGTTTTAATCTCTAACGAGGGAGATTCAC TGCCTTAGT	This study

TABLE 3 Mean diameter of phage plaques (mm)

Host Phage	B834	MG1655	BL21 (DE3)	BL21 (DE3) pET11aRIII	BL21 (DE3) pET11a RIII-H42R	BL21 (DE3) pTB146	BL21 (DE3) pTB146- nT
T4D	0.57 (±0.04)	0.67 (±0.04)	0.63 (±0.06)	0.53 (±0.05)	0.57 (±0.05)	0.68 (±0.04)	1.07 (±0.05)
T4rIII	1.09 (±0.09)	1.43 (±0.07)	1.07 (±0.09)	0.62 (±0.03)	0.92 (±0.08)	1.32 (±0.08)	1.38 (±0.06)
T4ΔrIII	0.92 (±0.08)	1.12 (±0.06)	0.95 (±0.07)	0.52 (±0.06)	0.86 (±0.08)	1.13 (±0.08)	1.17 (±0.07)
T4ΔrI	1.29 (±0.09)	1.88 (±0.11)	1.24 (±0.07)	1.21 (±0.03)	1.34 (±0.06)	-	-
T4rBB9	0.89 (±0.15)	-	-	-	-	-	-
T4rES35	1.02 (±0.05)	-	-	-	-	-	-
T4rES40	1.05 (±0.05)	-	-	-	-	-	-

Figure 1

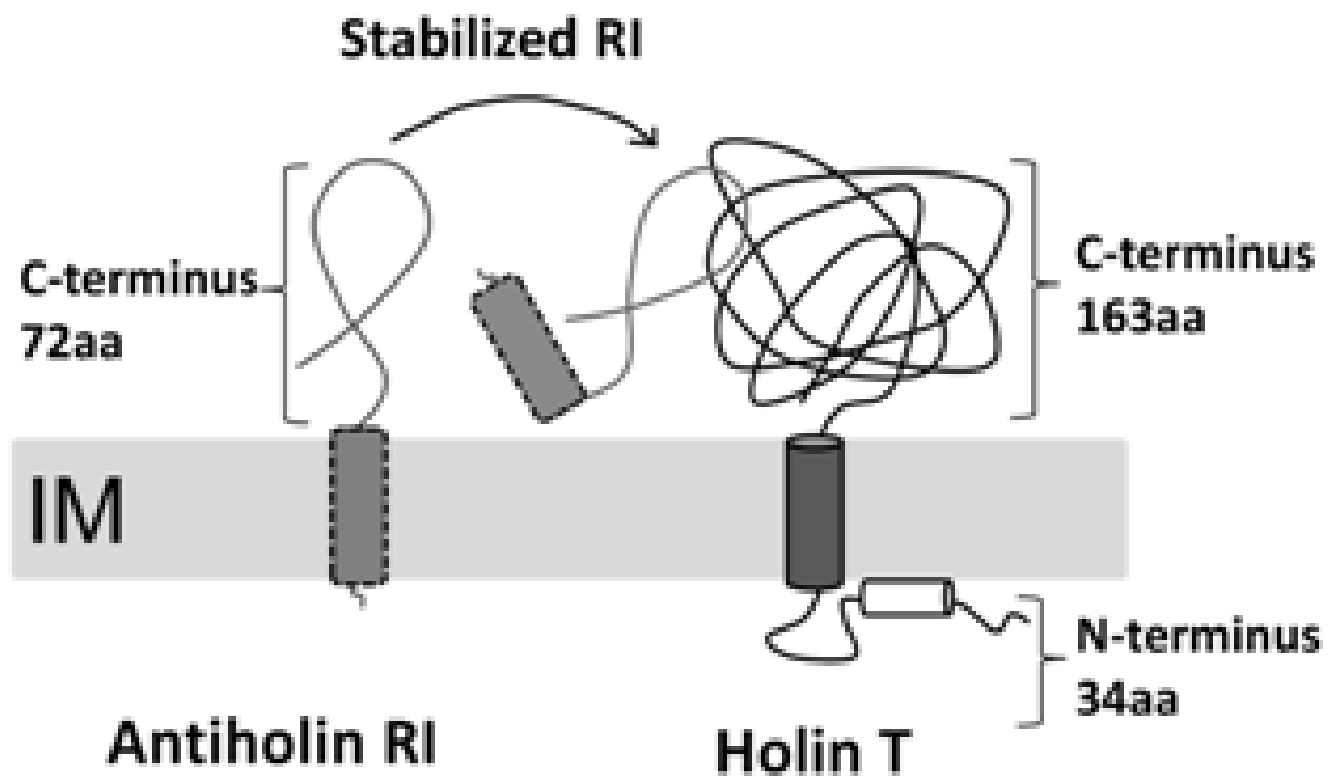


Figure 2

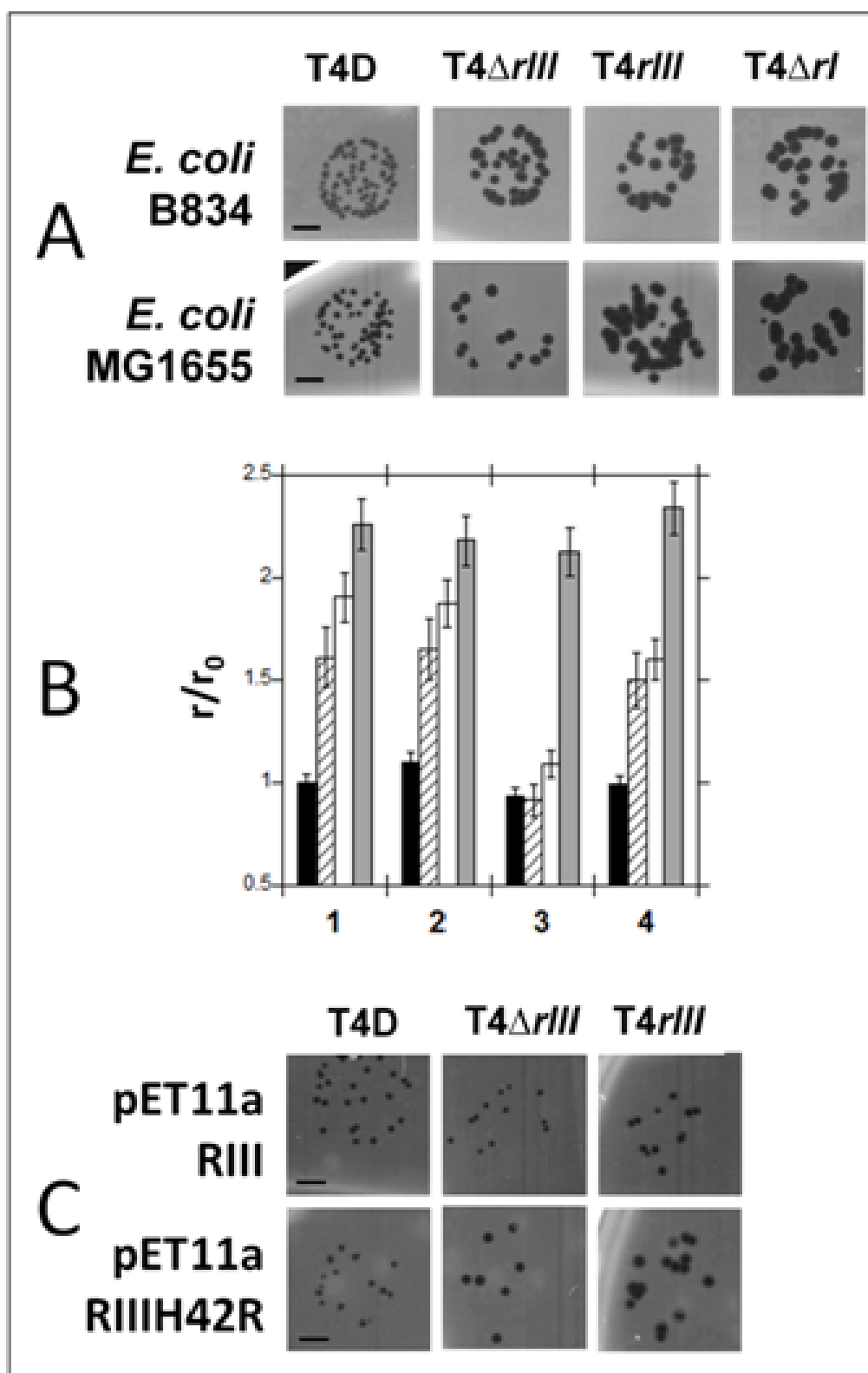


Figure 3

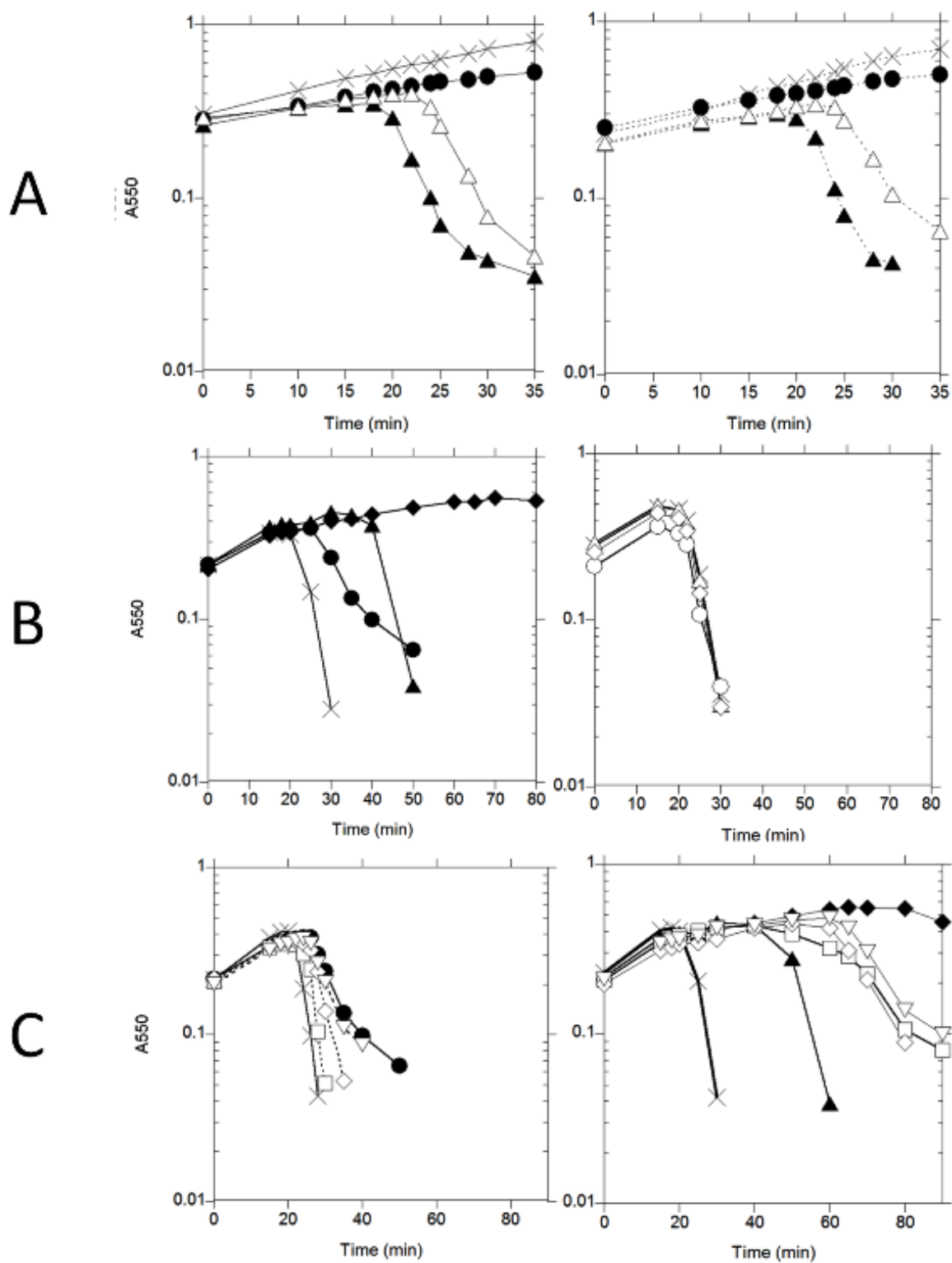


Figure 5

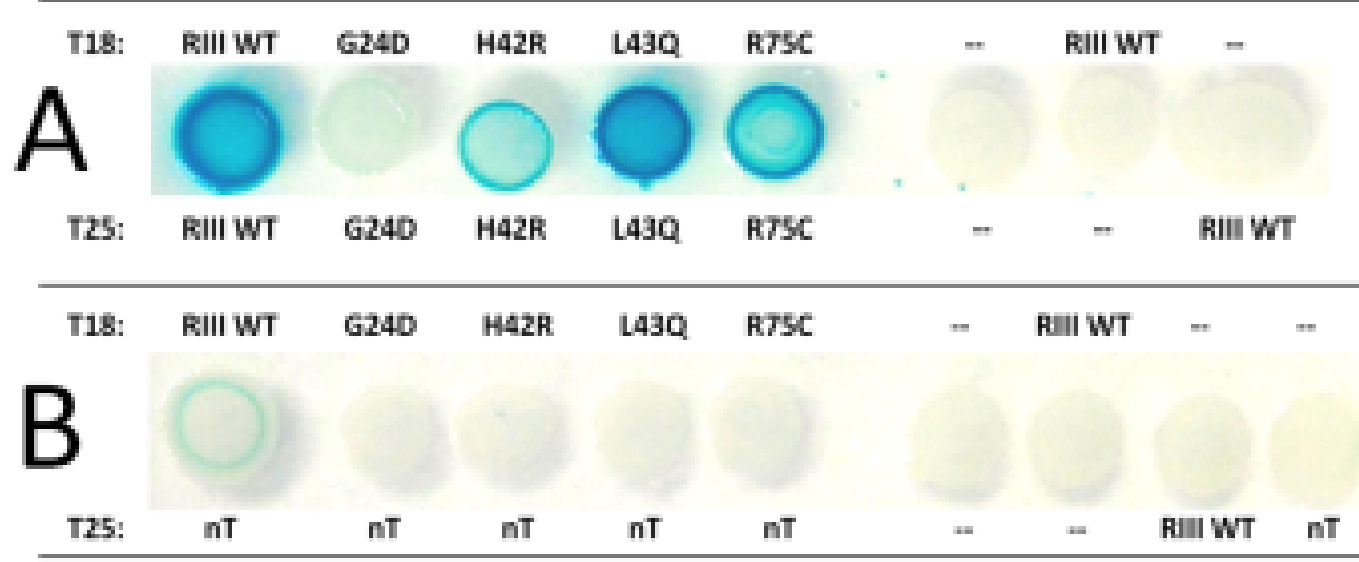


Figure 6

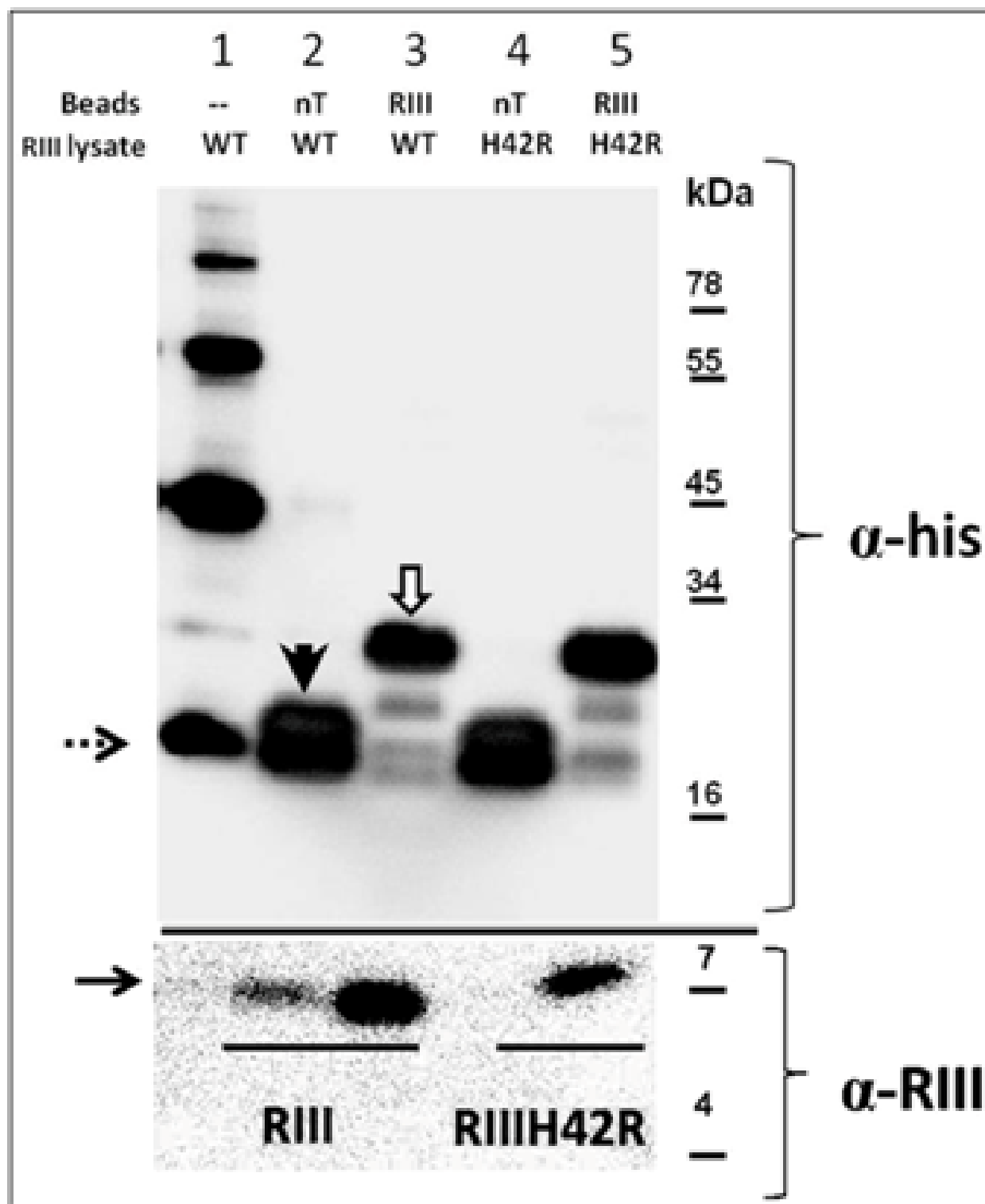


Figure 7

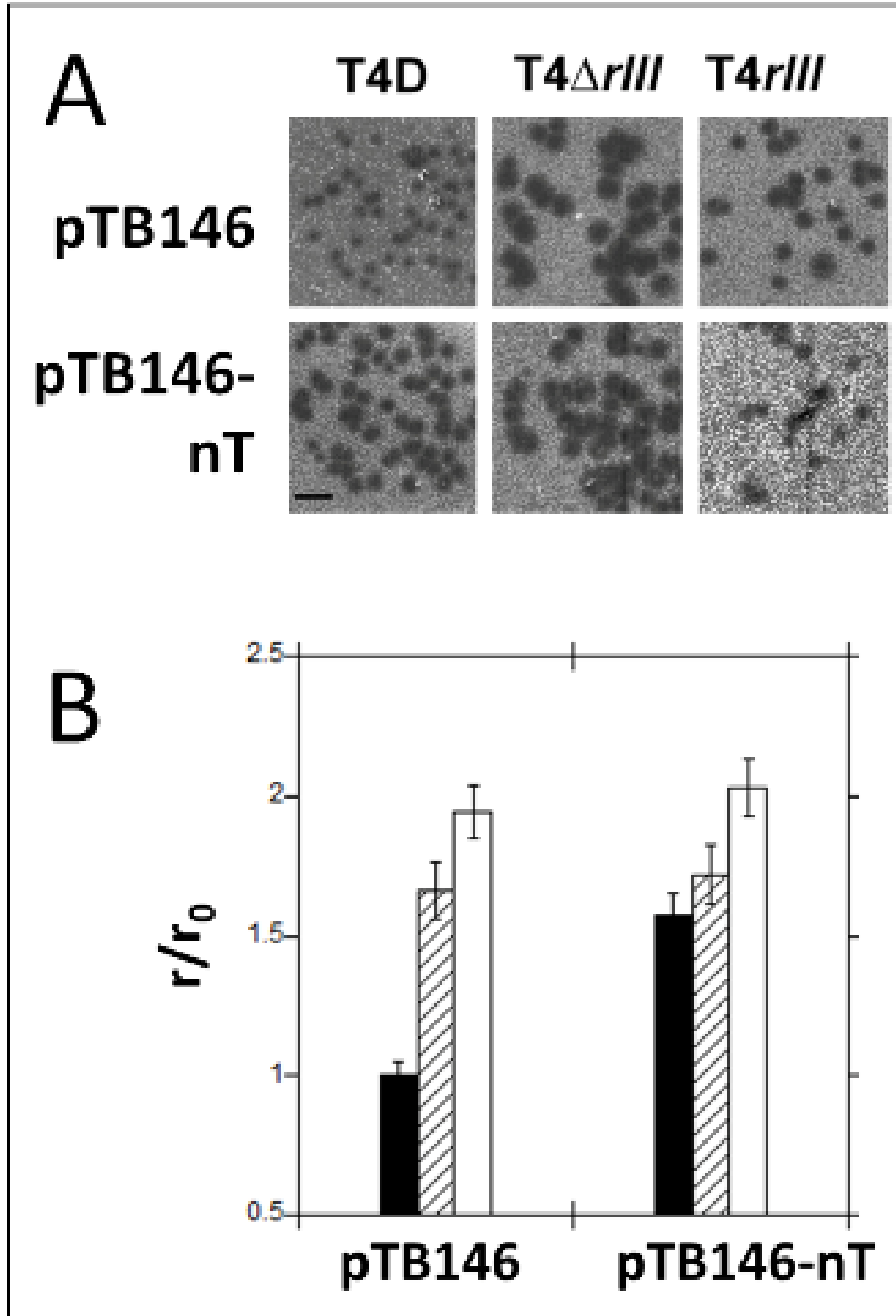


Figure 8

